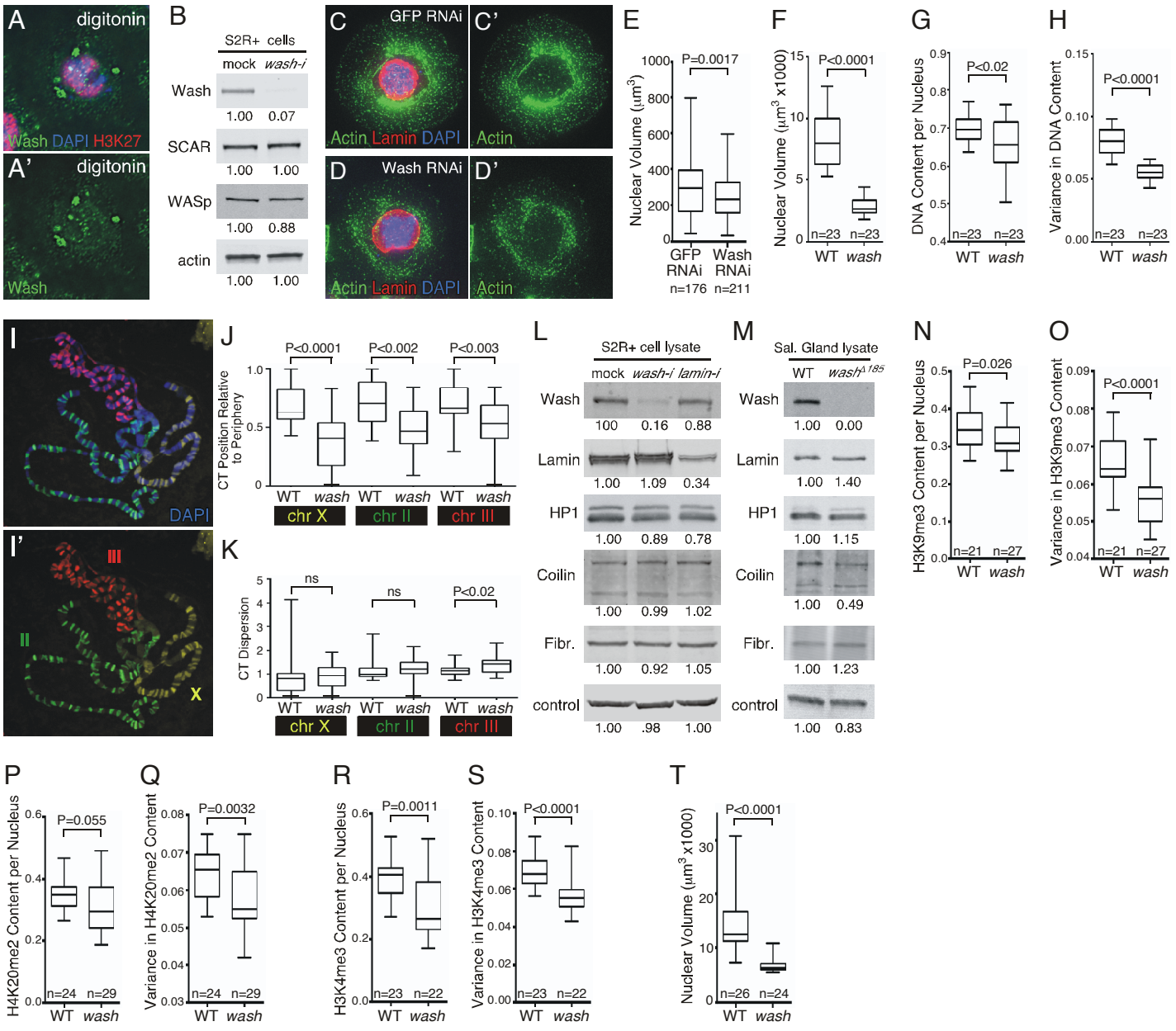
A
digitonin
Wash DAPI H3K27
A'
digitonin
Wash
B
S2R+ cells
mock wash-i
Wash
1.00 0.07
SCAR
1.00 1.00
WASp
1.00 0.88
actin
1.00 1.00
C
GFP RNAi
C'
Actin Lamin DAPI
Actin
D
Wash RNAi
D'
Actin Lamin DAPI
Actin
E
Nuclear Volume (μm3)
P=0.0017
GFP RNAi
Wash RNAi
n=176 n=211
F
Nuclear Volume (μm3 x1000)
P<0.0001
n=23 n=23
WT wash
G
DNA Content per Nucleus
P<0.02
n=23 n=23
WT wash
H
Variance in DNA Content
P<0.0001
n=23 n=23
WT wash
I
DAPI
I'
III
II
X
J
CT Position Relative to Periphery
P<0.0001
P<0.002
P<0.003
WT wash WT wash WT wash
chr X
chr II
chr III
K
CT Dispersion
ns
ns
P<0.02
WT wash WT wash WT wash
chr X
chr II
chr III
L
S2R+ cell lysate
mock wash-i lamin-i
Wash
100 0.16 0.88
Lamin
1.00 1.09 0.34
HP1
1.00 0.89 0.78
Coilin
1.00 0.99 1.02
Fibr.
1.00 0.92 1.05
control
1.00 .98 1.00
M
Sal. Gland lysate
WT wash Δ185
Wash
1.00 0.00
Lamin
1.00 1.40
HP1
1.00 1.15
Coilin
1.00 0.49
Fibr.
1.00 1.23
control
1.00 0.83
N
H3K9me3 Content per Nucleus
P=0.026
n=21 n=27
WT wash
O
Variance in H3K9me3 Content
P<0.0001
n=21 n=27
WT wash
P
H4K20me2 Content per Nucleus
P=0.055
n=24 n=29
WT wash
Q
Variance in H4K20me2 Content
P=0.0032
n=24 n=29
WT wash
R
H3K4me3 Content per Nucleus
P=0.0011
n=23 n=22
WT wash
S
Variance in H3K4me3 Content
P<0.0001
n=23 n=22
WT wash
T
Nuclear Volume (μm3 x1000)
P<0.0001
n=26 n=24
WT wash

Figure S1

Figure S1. Wash knockdown affects nuclear organization. Related to Figures 1 and 2.

(A-A') Controls for differential permeabilization with digitonin and triton-X100. Nuclear Wash (A-A') and H3K27me3 (A) staining are detected in S2R+ cells treated with 20mg/ml digitonin (a concentration of digitonin sufficient to permeabilize both the plasma and nuclear membranes). (B) Wash dsRNA targeted regions specifically deplete Wash protein in S2R+ cells. Western analysis of protein extracts from mock (GFP RNAi) and Wash RNAi S2R+ cells probed with antibodies recognizing Wash, WASp, SCAR, or a actin (loading control). The normalized levels of protein are indicated (with control set to 1.0). Wash depletion does not affect the expression of the related WASp or SCAR proteins. (C-D') Actin architecture in *wash* knockdown cells. Confocal projections of S2R+ cells treated with dsRNA for GFP (C-C') or Wash (D-D') then stained for Lamin (C, D), actin (C-D') and DNA (DAPI; C, D) showing that while cytoplasmic actin architecture is somewhat disrupted in Wash knockdown cells, it does not deform the nucleus. (E-F) Wash knockdown cells (E) and *wash* mutants (F) exhibit reduced nuclear volume. Quantification of nuclear volume in GFP dsRNA (292±11 μm^3; n=176) or Wash dsRNA (248±8 μm^3; n=211) treated S2R+ cells (P=0.0017) (E) and wildtype (8243±473 μm^3; n=23) or $wash^{\Delta 185}$ (2797±146 μm^3; n=23) salivary gland nuclei (P<0.0001) (F). Boxplot graphs show the median and 25% and 75% percentile measures. The whiskers indicate variability outside the upper and lower quartiles. (G-H) *wash* mutants exhibit lower DNA content in polytene salivary gland nuclei. This decrease is indicated by the quantification of the average DNA content in wildtype (0.7±0.01; n=23) and $wash^{\Delta 185}$ (0.66±0.01; n=23) salivary gland nuclei (P<0.02) (G) and by the variance in the DNA content in wildtype (0.08±0.01; n=23) and $wash^{\Delta 185}$ (0.06±0.01; n=23) salivary gland nuclei (P<0.0001) (H). Boxplot graphs show the median and 25% and 75% percentile measures. The whiskers indicate variability outside the upper and lower quartiles. (I-I') Fluorescent *in situ* hybridization of wildtype salivary gland polytene chromosome spreads with chromosome specific BAC pools for the X (yellow), second (green), and third (red) chromosomes. DNA is visualized by DAPI (I). (J-K) Chromosome Territories (CT) are disrupted in $wash^{\Delta 185}$ mutants compared to wildtype. Quantification of CT position relative to the nuclear periphery (J) and CT dispersion (K) (n=23 for each condition). CT position (0 signifies the periphery; 1 signifies the nucleus center): X chromosome: wildtype – 0.63, $wash^{\Delta 185}$ – 0.40, P<0.0001; Chromosome 2: wildtype – 0.71, $wash^{\Delta 185}$ – 0.47, P<0.002; and Chromosome 3: wildtype – 0.80, $wash^{\Delta 185}$ – 0.53, P<0.003. CT dispersion: X chromosome: wildtype – 0.54, $wash^{\Delta 185}$ – 0.93, P<0.31; Chromosome 2: wildtype – 0.99, $wash^{\Delta 185}$ – 0.1.21, P=0.13; and Chromosome 3: wildtype – 1.14, $wash^{\Delta 185}$ – 1.42, P<0.02. (L-M) Western analysis showing the relative levels of nuclear markers in mock (GFP RNAi) versus *wash* and *lamin* RNAi knockdown S2R+ whole cell extract (L) or wildtype versus $wash^{\Delta 185}$ salivary gland lysate (M). The normalized levels of protein are indicated with control (actin) set to 1.0. (N-S) Quantification of histone modifications in wildtype and $wash^{\Delta 185}$ salivary gland nuclei. Average H3K9me3 content in wildtype (0.35±0.01; n=21) and $wash^{\Delta 185}$ (0.32±0.01; n=27) salivary gland nuclei normalized to nuclear size (P=0.026) (N) and by the variance in the DNA content in wildtype (0.066±0.002; n=21) and $wash^{\Delta 185}$ (0.055±0.001; n=27) salivary gland nuclei (P<0.0001) (O). Average H4K20me2 content in wildtype (0.35±0.01; n=24) and $wash^{\Delta 185}$ (0.31±0.02; n=29) salivary gland nuclei normalized to nuclear size (P=0.055) (P) and by the variance in the DNA content in wildtype (0.064±0.001; n=24) and $wash^{\Delta 185}$ (0.057±0.001; n=29)

salivary gland nuclei (P=0.0032) (Q). Average H3K4me3 content in wildtype (0.40±0.01; n=23) and *wash*$^{\Delta 185}$ (0.31±0.02; n=22) salivary gland nuclei normalized to nuclear size (P=0.0011) (R) and by the variance in the DNA content in wildtype (0.069±0.002; n=23) and *wash*$^{\Delta 185}$ (0.057±0.002; n=22) salivary gland nuclei (P<0.0001) (S). Boxplot graphs show the median and 25% and 75% percentile measures. The whiskers indicate variability outside the upper and lower quartiles. (T) Specific disruption of nuclear Wash results in nuclear phenotypes. Quantification of nuclear volume in *wash*$^{\Delta 185}$ P{GFP-Wash^{WT}} (WT: 14093±958 μm^3; n=26) or *wash*$^{\Delta 185}$ P{GFP-Wash$^{+NES\Delta NLS}$} (ΔNLS: 6837±313 μm^3; n=24) transgenic salivary gland nuclei (P<0.0001). Boxplot graph shows the median and 25% and 75% percentile measures. The whiskers indicate variability outside the upper and lower quartiles.

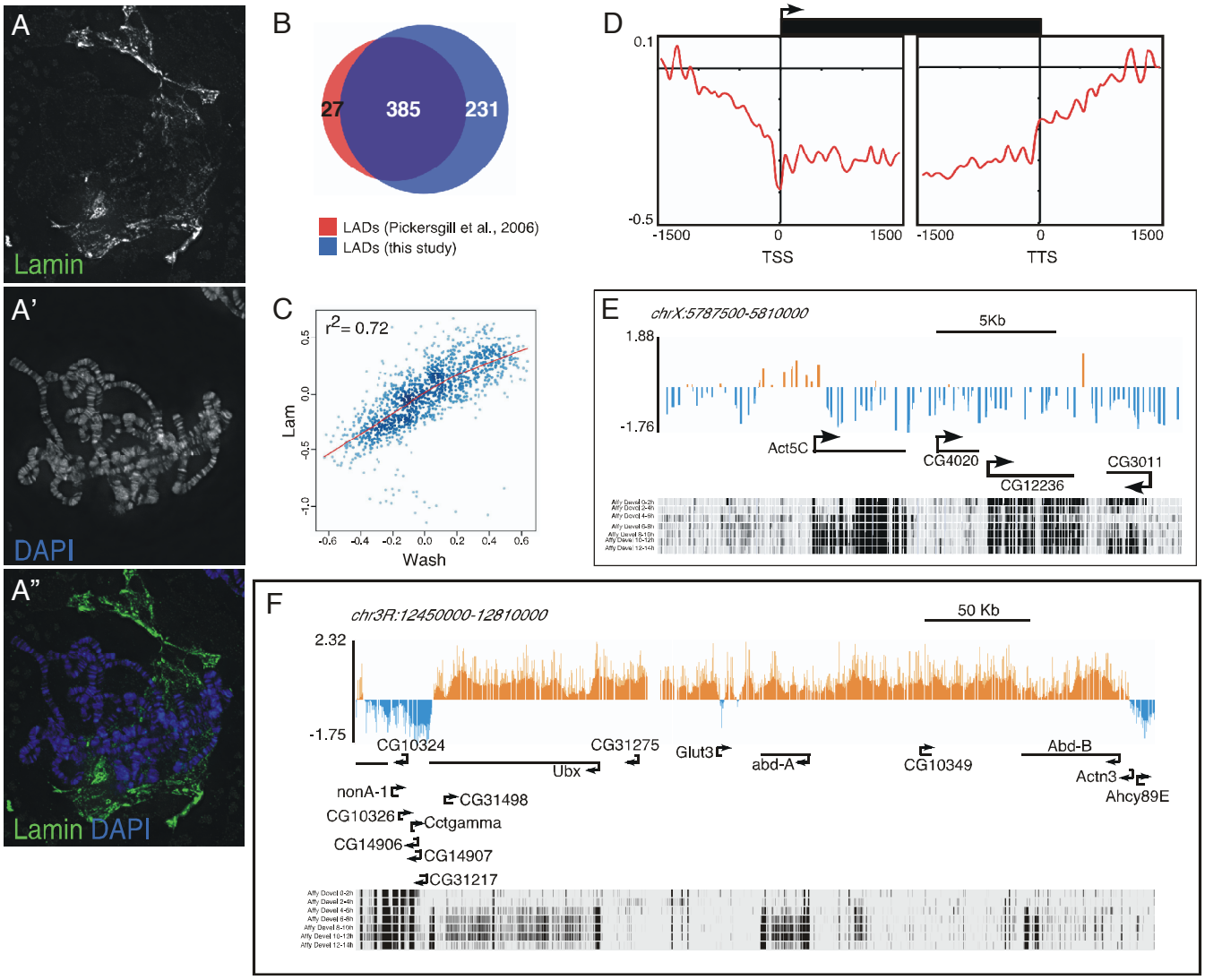
A
Lamin
A'
DAPI
A"
Lamin DAPI
B
27
385
231
LADs (Pickersgill et al., 2006)
LADs (this study)
C
r2= 0.72
Lam
Wash
D
0.1
-0.5
-1500
0
1500
TSS
TTS
E
chrX:5787500-5810000
5Kb
1.88
-1.76
Act5C
CG4020
CG12236
CG3011
F
chr3R:12450000-12810000
50 Kb
2.32
-1.75
CG10324
Ubx
CG31275
Glut3
abd-A
CG10349
Abd-B
Actn3
Ahcy89E
nonA-1
CG31498
CG10326
Cctgamma
CG14906
CG14907
CG31217

Figure S2

Figure S2. Wash associates with LADs. Related to Figure 3.

(A-A'') Lamin associates with the nuclear envelope, but not with polytene chromosomes. (B) Lamin DamID reproducibility. Venn diagram showing overlap between LADs generated in this study to those generated by Pickersgill et al., 2006. Our analysis identified 93.4% of the initially identified LADs ($P<1x10^{-6}$). (C) Correlation graph between LADs and Wash bound regions. Hidden Markov generated domains for Wash and Lamin exhibit a correlation coefficient of 0.72. (D) Depletion of Wash along gene bodies. To establish Wash distribution at coding regions, Drosophila genes were aligned at their transcriptional start site (TSS) and transcriptional termination sites (TTS) (+/- 1.5 Kb) and the normalized DamID probe signals were averaged in 150-bp bins. (E-F) Genome browser Snapshot showing the distribution of Wash in the constitutively expressed Act5C locus (E) and the developmentally regulated Bithorax Complex (F) in Kc cells. The Wash chromatin profile was expressed as smoothed DamID signal averaged for three independent experiments. Importantly, modENCODE RNAseq data shows that besides the non-coding *bxd* gene, the rest of the Bithorax Complex genes are not expressed in Kc167 cells (data not shown). The positions and the coding sequence gene structure of annotated transcripts are shown.

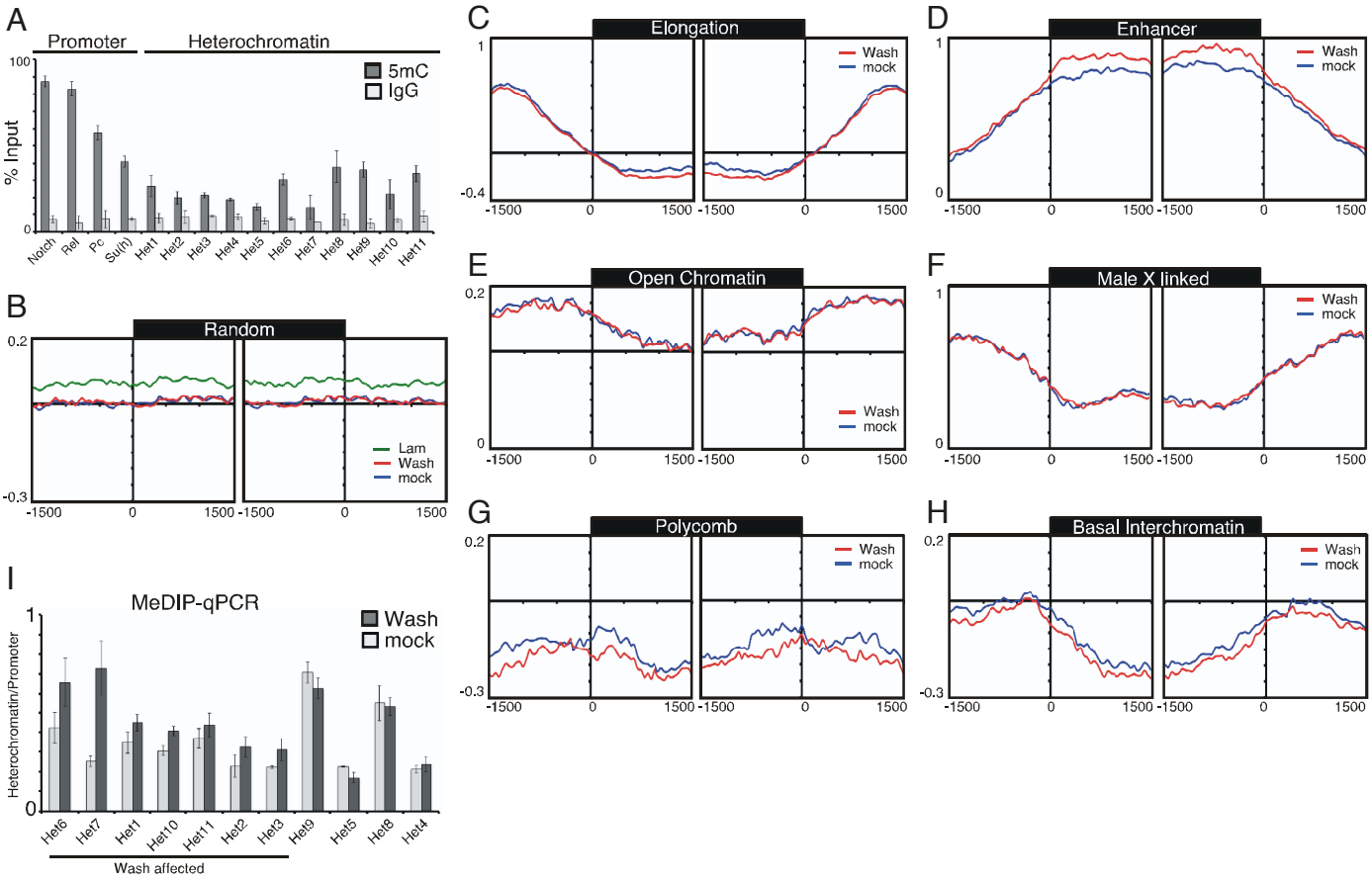
A
Promoter
Heterochromatin
5mC
IgG
% Input
Notch
Rel
Pc
Su(fl)
Het1
Het2
Het3
Het4
Het5
Het6
Het7
Het8
Het9
Het10
Het11
B
Random
Lam
Wash
mock
C
Elongation
D
Enhancer
E
Open Chromatin
F
Male X linked
G
Polycomb
H
Basal Interchromatin
I
MeDIP-qPCR
Heterochromatin/Promoter
Wash affected

Figure S3

Figure S3. Wash regulates chromatin accessibility of heterochromatic regions. Related to Figure 4.

(A) Validation of M.SssI-based chromatin accessibility by MeDIP-qPCR. Methylated DNA was immunoprecipitated with a non-specific or an anti-5methyl cytosine antibody. Specific primer sets for promoter (Notch, Rel, Pc, and Su(H)) and for 11 heterochromatin regions were used (see Supplemental Experimental Procedures for primer list). (B) A cohort of 6000 random regions was used to establish the global background methylation signal upon mock, Wash, and Lamin knockdown. Lamin exhibited a higher global non-specific background than either Wash or mock. (C-H) Distribution of M.SssI-based chromatin accessibility around elongating, enhancer, open chromatin, male X liked genes, Polycomb and basal interchromatic regions. Chromatin states generated by the modENCODE consortium were aligned at their 5' and 3' ends (+/- 1.5 Kb) and the normalized probe signals were averaged in 50-bp bins. Statistical significance was obtained by applying a non-parametric test (two sample Kolmogorov–Smirnov (KS) test) on the average number of normalized signal within 1.5 kb downstream of the 5' or upstream of the 3' of each region. While chromatin accessibility upon Wash knockdown was highly statistically significant at heterochromatin regions ($P<2\times10^{-3}$), Polycomb ($P<4\times10^{-3}$), BIC ($P<4x10^{-4}$), enhancer ($P<9x10^{-15}$), and elongation ($P<2\times10^{-8}$), other groups showed no significant change (i.e., HLE P=0.256, OC P=0.615, MXG=0.4135, Promoter (TSS)=0.8235, Random p=0.615). Unlike Wash, Lamin RNAi caused significant alterations in chromatin accessibility in all the tested chromatin states (Promoter= $P<4\times10^{-4}$, HLE $P<2x10^{-3}$, Heterochromatin $P<4x10^{-3}$). (I) MeDIP-qPCR of primer sets for heterochromatic regions described in (a) upon mock or Wash knockdown in S2R+ cells. The fold enrichment of heterochromatin is expressed as a ratio to promoter regions, as no change in promoter accessibility was observed in the meta-analysis (Figure 4A).

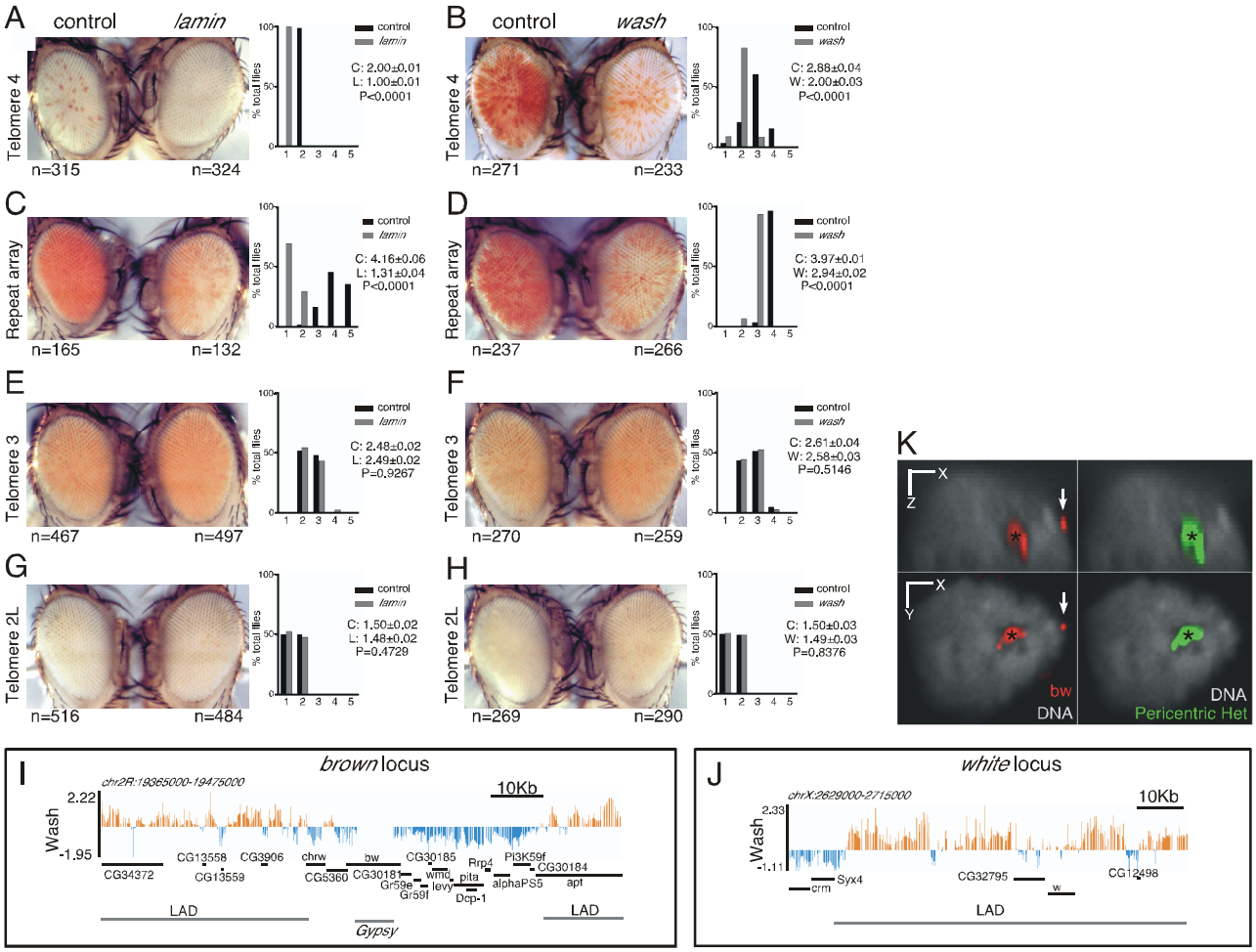
A
control
lamin
Telomere 4
n=315
n=324
C: 2.00±0.01
L: 1.00±0.01
P<0.0001
B
control
wash
Telomere 4
n=271
n=233
C: 2.88±0.04
W: 2.00±0.03
P<0.0001
C
Repeat array
n=165
n=132
C: 4.16±0.06
L: 1.31±0.04
P<0.0001
D
Repeat array
n=237
n=266
C: 3.97±0.01
W: 2.94±0.02
P<0.0001
E
Telomere 3
n=467
n=497
C: 2.48±0.02
L: 2.49±0.02
P=0.9267
F
Telomere 3
n=270
n=259
C: 2.61±0.04
W: 2.58±0.03
P=0.5146
G
Telomere 2L
n=516
n=484
C: 1.50±0.02
L: 1.48±0.02
P=0.4729
H
Telomere 2L
n=269
n=290
C: 1.50±0.03
W: 1.49±0.03
P=0.8376
% total flies
control
lamin
wash
K
X
Z
Y
bw
DNA
DNA
Pericentric Het
I
brown locus
chr2R:19365000-19475000
10Kb
Wash
2.22
-1.95
CG34372
CG13558
CG13559
CG3906
chrw
CG5360
bw
CG30185
CG30184
LAD
Gypsy
J
white locus
chrX:2629000-2715000
10Kb
Wash
2.33
-1.11
Syx4
crm
CG32795
CG12498
w
LAD

Figure S4

Figure S4. Wash and Lamin differentially affect *brown*- and *white*-based Position Effect Variegation. Related to Figure 4.

(A-D) *wash* and *lamin* enhance *white* mediated heterochromatic PEV. Wash and Lamin mediate enhancement of w^+ gene inserted in near the telomere on chromosome 4 (A-B) and within a repeat-array (C-D), both of which are affected by the heterochromatic silencing machinery. (E-H) *wash* and *lamin* do not affect telomeric PEV. Wash and Lamin do not affect w^+ gene expression when inserted near Telomere 3 (E-F) or Telomere 2L (G-H). Bar plots show percentage of flies falling into each expression quintile (flies sorted into one of five bins based on the percentage of ommatidia expressing the w^+ marker or the *bw* gene (bin 1 = 0-20% to bin 5 = 80-100%). The median±SEM and P-values are given in each panel. Eyes shown are representative of the average phenotype for each genotype and each pair is an age-matched, sibling pair. The number of eyes scored (N) is given below each eye. L=*lamin*, W=*wash*, and C=sibling control. (I-J) Wash chromatin profile on genomic regions of chromosome 2R and chromosome X containing the *bw* (I) and *w* (J) loci, respectively. Gene coding sequences are shown as black lines. Wash/LADs regions are indicated in gray. The presence of a gypsy transposon inserted in the *bw* gene is also indicated. (K) Fluorescent *in situ* hybridization of a BAC containing the *bw* gene (red) in S2R+ cells confirms the peripheral localization of the *bw* locus (arrow). The presence of the gypsy transposon in this BAC also labels the pericentric heterochromatin as confirmed with the use of specific oligo probe (green).

Supplemental Experimental Procedures

Fly stocks

Flies were cultured and crossed at 25°C on yeast-cornmeal-molasses-malt medium. The following stocks were used: OregonR (wildtype) [S1], *wash*$^{\Delta 185}$ [S2], and *lam*^{sz18} [S3]. The PEV lines used are as follows: pericentromeric – ln(1)w^{m4}, w^{m4e} (provided by S. Henikoff); repeat array – w^{1118}; P[lacW]FX1/CyO (provided by S. Henikoff); telomeric – Telomere 2L- 39C•5, Telomere 3R-39C•55, and Telomere 4-39C•72 (provided by L. Wallrath); and *bw* based – *bw*^{D}*; st* and *In(2R)bw*^{VDe}*/SM1; st* (provided by S. Henikoff).

Construction of the GFP-Wash$^{+NES\Delta NLS}$ and GFP-Wash^{WT} transgenic lines

A 2.9 kb genomic fragment encompassing the entire Wash gene was PCR'd, then subcloned into the Casper 4 (C4) transformation vector by adding KpnI (5') and BamHI (3') restriction sites. GFP was inserted N-terminal to the Wash ATG by PCR. Since Wash is known to interact with other proteins that have a nuclear localization sequence, we also added a strong canonical Nuclear Export Signal (+NES: LDELLELLRL) inserted N-terminal to the GFP by PCR. Wash's Nuclear Localization Signal (NLS) was disrupted by a 4 amino acid substitution mutation generated by PCR (ΔNLS: WKRS>AAAA; aa197-200) to yield C4-GFP-Wash$^{+NES\Delta NLS}$. A control construct was also generated that contained the GFP fusion, but lacked the +NES or ΔNLS changes (C4-GFP-Wash^{WT}).

These two constructs were used to make germline transformants as previously described [S4]. Transgenic lines that mapped to Chromosome 2 and that had non-lethal insertions were kept. The resulting transgenic lines (P{*w*$^{+}$; *GFP-Wash*^{WT}} and P{*w*$^{+}$; *GFP-Wash*$^{+NES\Delta NLS}$}) were recombined onto the *wash*$^{\Delta 185}$ null chromosome to assess the contribution of the particular Wash transgene. The resulting recombinants (*wash*$^{\Delta 185}$ P{*w*$^{+}$; *GFP-Wash*^{WT}} and *wash*$^{\Delta 185}$ P{*w*$^{+}$; *GFP-Wash*$^{+NES\Delta NLS}$}) are essentially gene replacements, as *wash* activity is only provided by the transgene. These transgenes do not rely on over-expression, but rather on the spatial and temporal expression driven by the endogenous *wash* promoter itself. We analyzed a minimum of three lines per construct and have checked all lines to confirm that the levels and spatial distribution of their expression is indistinguishable from wildtype. The wildtype version of this transgene (*wash*$^{\Delta 185}$ P{ *w*$^{+}$; *GFP-Wash*^{WT}}) rescues the lethality associated with the *wash*$^{\Delta 185}$ loss of function mutation and can be maintained as a stock.

Position Effect Variegation

We examined the effects of *wash*$^{\Delta 185}$ and *lamin*^{sz18} on both classical (*w*^{m4}, *bw*^{VDe2}; variably silenced because of their position next to heterochromatin) and non-classical (*bw*^{D}; variably silenced, but not due to gross chromosomal rearrangements) PEV mutations [S5-S8]. PEV reporter line females were crossed to *wash*$^{\Delta 185}$*/CyO* or *lam*^{sz18}*/CyO* males then reporter line/*wash*$^{\Delta 185}$ or reporter line/*lam*^{sz18} progeny and reporter line/CyO sibling progeny controls were scored. At least 200 progeny from each cross were analyzed when progeny were 4 days old to allow for pigmentation to be completed. Flies were sorted by genotype (and in some cases, gender) then classified into one of five bins based on the percentage of ommatidia expressing the w^{+} marker (with bin 1 being 0-20% of ommatidia expressing red pigment to bin 5 being 80-

100% of ommatidia expressing red pigment). For *white*-based PEV reporters, only male progeny are shown. For *brown*-based PEV reporters, both males and females are shown. The average phenotype is represented.

dsRNA production

To generate the Wash and Lamin double strand RNA (dsRNA), the template was amplified by PCR using primers that include the T7 promoter sequence. For Wash, 2 sequences were used: RNAi#1, a 495 base-pair region (CTGGCCTGGGCATCCT to AAGGACATTGTCCCACACTC) and RNAi#2, a 427 base-pair region (ATGGAGGAGTCACCTTAC to ACATGGAAAAAGATGTCCGC) with no predicted off-targets was identified by SnapDragon (www.fly**rna**i.org/**snapdragon**). For Lamin dsRNA generation, a 310 base-pair region (GCGGCTAATCAACGAGAAAG to GTAGAGCTGCTCATTGCCGT) with no predicted off-targets. For control (GFPi) dsRNA generation, a 520 base-pair region (GGCACAAATTTTCTGTCAGT to TCTGGTAAAAAGGACAGGGCC) was used. dsRNA was synthesized using a MEGAscript RNAi Kit (Ambion, AM1626) according to manufacturer's instructions.

Cell culture and RNAi treatment

Kc167 and S2R+ cells were grown at 25°C in a humidified incubator. Kc167 cells were maintained in CCM3 media (HyClone) supplemented with L-glutamine, penicillin and streptomycin. S2R+ cells were grown in Schneider's media (Invitrogen) supplemented with 10% FBS and penicillin and streptomycin. 60 mg of dsRNA was added twice over 7 days to $2x10^6$ cells growing in 10 ml of media.

Immunostaining of salivary glands and S2 cells

Flies were transferred daily and wandering 3rd instar larvae were collected and subsequently dissected in cold PBS. Glands were fixed using 1:6 fix/heptane for 10 minutes. Fix is: 16.7 mM KPO_4 pH6.8, 75 mM KCl, 25 mM NaCl, 3.3 mM $MgCl_2$, 6% formaldehyde. After three washes with PTW (1× PBS, 0.1% Tween-20), salivary glands were permeabilized in 1× PBS plus 1% Triton X-100 for 2 hours at room temperature, then blocked using PAT (1× PBS, 0.1% Tween-20, 1% bovine serum albumin (BSA), 0.05% azide) for 2 hours at 4°C. Antibodies were added at the following concentrations: mouse anti-Wash monoclonal (P3H3; 1:150 dilution) [S9], mouse anti-Lamin monoclonal (ADL67.10; 1:100 dilution; Developmental Studies Hybridoma Bank), anti-HP1 monoclonal (C1A9-s; 1:100 dilution; Developmental Studies Hybridoma Bank), mouse anti-fibrillarin monoclonal (72B9; 1:5 dilution) [S10], rabbit anti-Coilin (R#1; 1:2000 dilution) [S11], rat anti-Mtor and rabbit anti-Mof (1:500 dilution) [S12], anti-actin monoclonal (Clone C4; 1:10,000 dilution; MP Biochemicals), rabbit anti-GFP (A11122; 1:1000 dilution; Molecular Probes/Invitrogen); rabbit anti-H3 (39163; 1:1000 dilution; Active Motif), rabbit anti-H3K27me3 (07-449; 1:1000 dilution; EMD Millipore), rabbit anti-H3k4me3 (39159; 1:1000 dilution; Active Motif), rabbit anti-H3K9me3 (ab8898; 1:1000; Abcam), and rabbit anti-H4k20me2 (07-367; 1:1000 dilution, EMD Millipore), and the salivary glands were incubated overnight at 4°C. Primary antibody was then removed and glands were washed three times with XNS (1× PBS, 0.1% Tween-20, 0.1% BSA, 2% normal goat serum) for 30 min each. Alexa

conjugates secondary antibodies (Invitrogen) diluted in PbT (1:1000) were then added and the salivary glands were incubated overnight at 4°C. Salivary glands were washed 10 times with PTW at room temperature for 10 minutes each and were incubated for 15 minutes with DAPI (1μg/ml, to visualize DNA) after the fourth wash. Glands were mounted on slides in SlowFade Gold with DAPI media (Invitrogen) and visualized using a Zeiss confocal microscope as described below.

S2R+ cells were stained as previously described [S9]. Antibodies were added at the following concentrations: mouse anti-Wash monoclonal (P3H3; 1:100 dilution) [S9], mouse anti-Lamin monoclonal (ADL67.10; 1:50 dilution; Developmental Studies Hybridoma Bank), anti-alpha-tubulin monoclonal (DM1A; 1:2000 dilution; Sigma) and anti-actin monoclonal (Clone C4; 1:10,000 dilution; MP Biochemicals). DAPI (1 μg/ml) was used to visualize DNA.

Differential nuclear permeabilization was performed by incubating S2R+ cells with 5 mg/ml of digitonin in buffer B [20mM Hepes; 110 mM potassium acetate; 5 mM sodium acetate; 2 mM magnesium acetate; 1 mM EGTA; and added immediately before use: 2 mM DTT and protease inhibitors] for 3 min. Cells were then washed once with buffer B and two more times with PBS. Cells were fixed with 4% formaldehyde in PBS for 20 min at RT. Slides were blocked with PAT and stained with anti-Wash and anti-H3K27me3 as mentioned above. As a control, a concentration of 20 mg/ml digitonin was used to completely permeabilize both cytoplasmic and nuclear compartments.

Duolink Proximity Ligase Assays

Duolink Proximity Ligase assays (PLA) were performed with salivary glands from otherwise wildtype larvae expressing a GFP-Lamin (B-type) transgene. Glands were fixed, blocked, and incubated with antibodies recognizing Wash (mouse anti-Wash P3H3 monoclonal; 1:10 dilution; [S9]) and GFP (rabbit anti-GFP; 1:1000 dilution; Molecular Probes/Invitrogen) as described above. After washing, glands were incubated with secondary antibodies conjugated with Duolink PLA probes, followed by hybridization, ligation, and amplification according to manufacturer instructions (Sigma). *In situ* red Duolink signal is only generated if the two PLA probes are within 30-40 nm. Images were acquired using a Zeiss confocal microscope as described below.

Microscopy

The following microscopes were used in these studies:

i) DeltaVision RT microscope with a 100× Oil objective. The following filters were used: DAPI 360/40 457/40, FITC 490/20 526/38, RD-TR-Cy3 555/28 617/63.

ii) Zeiss LSM-510META confocal microscope with excitation at 488 nm or 543 nm and emission collection using a BP-505–550, BP-560–615 or LP-560 filter. For DAPI visualization we used a two-photon 780 nm laser line and a BP415–450 filter. Images were obtained using a Plan-Apochromat 20 times/0.75 dry objective.

iii) Zeiss LSM 780 spectral confocal microscope (Carl Zeiss Microscopy GmbH, Jena, Germany) fitted with a Zeiss 20x/0.8 Plan-Apochromat objective. DAPI fluorescence was excited with a 405 nm diode laser, and detection was between 413-485 nm. FITC (Alexa 488) fluorescence was excited with the 488 nm line of an Argon laser, and detection was between 498-560 nm. Red

(Alexa 568) fluorescence was excited with the 561 nm line of a DPSS laser and detection was between 570-670 nm. Pinhole was typically set to 1.0 Airy Units. Confocal sections were acquired at 0.5-1.0 micron spacing.

iv) UltraVIEW VoX Confocal Imaging System (PerkinElmer, Waltham, MA), in a Nikon Eclipse Ti stand (Nikon Instruments, Melville, NY), with 100× 1.4 NA objective lens and controlled by Volocity software (v.5.4.0, PerkinElmer, Waltham, MA). Images were acquired with 491 nm and 561 nm, with a Yokogawa CSU-X1 confocal spinning disc head equipped with a Hamamatsu C9100-13 EMCCD camera (PerkinElmer, Waltham, MA).

Microscope settings were optimized for control experiments and identical settings were used on experimental samples.

Quantitative 3D image analysis

Images were exported as TIFFs or LSM files and imported into ImageJ. Adjustments were matched between controls and experiments. 3D nuclei images were generated using Volocity (v.5.4.0, PerkinElmer, Waltham, MA). For quantitative analysis, representative volume renderings of nuclei and painted chromosome territories (CTs) were obtained using Imaris software (Imaris x64 v7.2.3, Bitplane Inc). Alterations in three-dimensional nuclear organization from wildtype (WT) and *wash* mutants of equivalent developmental stages and in the same region of the salivary gland (central portion) were quantified by automated 3D analysis of 4-color image stacks acquired with the confocal spinning disc microscope. The size of individual voxels in the 3D image was 0.142 x 0.142 x 0.5 microns. Twenty-three nuclei (see below) were analyzed for each condition. Nuclear size (volume), shape irregularity (measured as the extent of concavities in the nuclear envelope where nuclei without any surface abnormalities – spherical, elliptical, cylindrical – have value of 0), and DNA content (integrated nuclear intensity normalized by nuclear volume) were computed from the DAPI channel. Spatial chromosome territory (CT) organization of chromosomes 2, 3, and X was represented by two metrics - relative radial position of a CT (RRP_{CT}, adapted from Meaburn et al, 2009 [S13]), and the extent of dispersion of the CT in the nucleus ($Disp_{CT}$). RRP has a value of 1 if the CT is located at the nuclear center and 0 if it at the nuclear periphery. $Disp_{CT}$ for a given CT is measured as the normalized average distance between the geometric centroids of all disparate clumps that constitute the CT. The equivalent radius of the nucleus (radius of a sphere with same volume) is used as the normalizing factor. CT morphometrics were quantified from the respective chromosome paint images in the remaining 3 channels. Images were first enhanced using a power law transformation ($I_{out} = I_{in}^{\gamma}$, $\gamma = 4$ for DAPI channel, 3 for the channels of chromosome 2 and 3, and 2 for chromosome X channel). Thereafter, a custom adaptive intensity thresholding scheme was used to derive 3D binary masks for the nucleus and the 3 CTs. The threshold intensity value for each channel was set to the upper edge of the intensity histogram's mode for that channel. Post-threshold binary masks were refined by a morphological opening operation with a sphere of radius 3 followed by the removal of spurious objects using an empirically established size threshold. Incomplete nuclei touching the image borders were omitted from further analysis. All segmented masks were manually checked for correctness prior to computation of morphometrics. Lastly, the Kruskal-Wallis non-parametric test was applied to

identify statistically significant alterations between the measured morphological data of wildtype and *wash* mutant nuclei. This quantitative morphological analysis procedure was applied to two independent biological replicates and yielded similar trends between hybridizations (data for nuclei from >10 glands of one replicate are shown as representative results). Using our quality controls described before, 23 wildtype nuclei were analyzed and compared to 23 *wash* nuclei that were randomized from 32 quality acquisitions. Image processing and statistical analysis were accomplished using Matlab software (v2012a, Mathworks, Natick, MA).

Lamin clones, Protein Expression, Westerns, and GST pull-down Assays

Wash constructs used in this study were described previously [S2, S14]. For Lamin *in vitro* translation, the full length Lamin Dm0 cDNA (1-623 aa) was PCR amplified as an 5'*Eco*RI-3'*Bgl*II fragment that was then cloned into the 5'*Eco*RI-3'*Bam*HI sites of pCite4a+ to generate Cite-Lamin(FL). For Lamin protein expression, the full length Lamin Dm0 cDNA (1-623 aa) was PCR amplified as an 5'*Eco*RI-3'*Not*I fragment that was then cloned into the 5'*Eco*RI-3'*Not*I sites of a modified 'double-tag' pGEX [S2] to generate dt-Lamin(FL).

Protein expression, purification, westerns, and GST pull-down assays were performed as previously described [S2, S14, S15]. Antibodies used for western blots are as follows: anti-Wash monoclonal (P3H3; 1:25 dilution)[S9], anti-Lamin monoclonal (ADL67.10; 1:500 dilution for cells; 1:100 dilution for salivary glands; Developmental Studies Hybridoma Bank), anti-SCAR monoclonal (P1C8; 1:250 dilution) [S9], anti-WASp monoclonal (P5C1; 1:25 dilution) [S9], rabbit anti-fibrillarin (ab5821; 1:1000 dilution; Abcam), anti-HP1 monoclonal (C1A9-s; 1:100 dilution; Developmental Studies Hybridoma Bank), rabbit anti-Coilin (R#1; 1:500 dilution) [S11], anti-actin monoclonal (Clone C4; 1:10,000 dilution; MP Biochemicals), rabbit anti-H3 (39163; 1:2000 dilution; Active Motif), rabbit anti-H3K27me3 (07-449; 1:1000 dilution; EMD Millipore), rabbit anti-H3k4me3 (39159; 1:1000 dilution; Active Motif), rabbit anti-H3K9me3 (ab8898; 1:1000; Abcam), rabbit anti-H4k20me2 (07-367; 1:1000 dilution, EMD Millipore), goat anti-mouse IgG (IRDye800CW; 1:15,000 dilution; LI-COR), goat anti-Rabbit IgG [H+L] (IRDye680LT; 1:15,000 dilution; LI-COR), and donkey anti-mouse, anti-rabbit, anti-rat, and anti-guinea pig HRP (1:15,000 dilution; Jackson ImmunoResearch).

Lysates and histone preparation

Drosophila 0-2 hour embryo whole cell extracts (WCE) and 0-12 hour embryo nuclear extracts (NE) were a gift from T. Tsukiyama (FHCRC). For total protein extractions, S2R+ cells or Drosophila larvae were resuspended in RIPA buffer with protease and phosphatase inhibitors. Nuclei were sonicated 5 times using a Sonic Dismembrator (Model 60; Fisher Scientific) at setting 4 with 5 seconds per pulse. The extract was spun at 16,000 xg for 10 min at 4°C and the supernatant recovered. For analyzing the chromatin-bound histones in S2R+ cells, cells were washed with PBS once, resuspended in NP-40/sucrose buffer (0.32 M Sucrose, 3 mM $CaCl_2$, 2 mM $MgCl_2$, 0.1 mM EDTA and 1.5% NP-40) and incubated on ice for 5 min. Nuclei were pelleted at 1500 xg and washed once with sucrose buffer without NP-40. For nuclear extracts, pelleted nuclei were washed once with sucrose buffer without NP-40 and resuspended in buffer BM (20 mM Hepes pH 7.4, 0.5 mM EDTA, 100 mM KCl, 10% glycerol, 2 mM DTT, 3 mM CaCl2, 1.5 mM MgCl2, 0.25 mM NaOVO3, 10 mM NaF, Protease inhibitors and 10 U of

MNase I) and incubated for 5 min at 37. Extract was incubated on ice for 30-60 min and spun at 12000 xg for 5 min at 4°C. Supernatant was transferred to a new tube and labeled as nuclear fraction. For histone fractionation, pelleted nuclei were treated as described [S16]. Histones were resuspended in water and quantified.

Immunoprecipitations

Lysates was incubated with primary antibody overnight at 4°C. Protein G sepharose (20 µl) was then added in 0.5 ml Carol Buffer (50 mM Hepes pH7.9, 250 mM NaCl, 10 mM EDTA, 1 mM DTT, 10% glycerol, 0.1% Triton X-100) + 0.5 mg/ml BSA + protease inhibitors (Complete EDTA-free Protease Inhibitor cocktail; Roche) and the reaction allowed to proceed for 2 hours at 4°C. The beads were washed 1x with Carol Buffer + BSA and 2x with Carol Buffer alone. Analysis was conducted using SDS-PAGE followed by Western blots. Antibodies used for immunoprecipitations are as follows: anti-Wash monoclonal (P3H3) [S9] and anti-9e10 (Developmental Studies Hybridoma Bank). Antibodies used for the IP western blots are as follows: anti-Wash monoclonal (P3H3; 1:200 dilution) [S9], anti-Lamin (ADL67.10; 1:20 dilution; Developmental Studies Hybridoma Bank), and goat anti-mouse HRP (1:15,000 dilution; Jackson ImmunoResearch Laboratories Inc.).

Polytene staining

Wildtype third instar larval salivary gland polytene chromosomes were prepared and stained for endogenous proteins as previously described [S17, S18]. Antisera used are as follows: polyclonal mouse anti-Wash (1:20 dilution) [S9]; monoclonal mouse anti-Lamin (mixture of 1:5 each of ADL67.10, ADL101, ADL84.14, ADL40; Developmental Studies Hybridoma Bank); and goat anti-mouse Alexa 488 (1:1000 dilution; Molecular Probes/Invitrogen). Chromosomes were viewed on a DeltaVision RT microscope equipped with a 40x/N.A. 1.35 oil immersion objective. 3-D stacks were collected using the DeltaVision softWoRx acquisition software (Applied Precision LLC, Issaquah, WA), and out of focus information was removed using a constrained iterative deconvolution algorithm [S19].

Fluorescent *In Situ* Hybridization (FISH)

Larvae were dissected in PBS and salivary glands were washed in PBS once and fixed in 6% EM-grade formaldehyde (Polysciences) diluted in PBS, with three times volume of heptane. Glands were permeabilized in 1% Triton in 1x PBS for 1 hour at room temperature (RT). After washing twice with PBT (PBS plus 0.1% Tween 20), glands were incubated with 0.2 mg/ml RNaseI in PBT for 2 hours at RT. Tissues were incubated in 0.1 M HCl for 10 min and treated for 45 sec with 25 µg/ml Pepsin A (3,070 u/mg; Worthington) in 0.1 M HCl. After washing once with PBT, the glands were fixed again with 6% formaldehyde diluted in PBS for 20 min at RT. Hybridization was performed as described in the Epigenome NoE protocol PROT07 (http://www.igh.cnrs.fr/equip/cavalli/Lab%20Protocols/p5.pdf) [S20]. After hybridization and post-hybridization washes, glands were incubated with 1 µg/ml DAPI in PBT for 30 and wash twice with PBT for 10 min at RT. For FISH in S2R+ cells, cells were incubated on Poly-L-Lysine coated slides and then followed the above protocol, except that the slides were treated for 30 sec with 50 µg/ml pepsin in 0.1 M HCl. Chromosome paint probes were a gift from A.

Minoda and G. Karpen [S21]. DNA was amplified using WGA2 (Sigma-Aldrich) and the DNA was labeled with the ARES DNA labeling kit (Alexa-488, 594 and 647) (Invitrogen). Alexa 594-labelled oligo complementary to pericentric heterochromatin was purchased from Invitrogen (seq: 5'-AACACAACACAACACAACACAACACAACACAACACAACAC)-3'. The BAC CH322-113J1 was used to identify the *bw* locus (BACPAC Resources Center, Children's Hospital Oakland Research Institute).

For FISH on polytene squashes, salivary glands were incubated in 45% acetic acid for 3 min. Tissues was transferred to lactic acid solution (1:1 - Lactic acid/60% acetic acid) on a coverslip. The tissue was squashed on a clean glass slide, incubated for 20 sec in liquid nitrogen then transferred to pre-chilled 100% ethanol. Chromosomal DNA was denatured in 0.1M HCl for 10 min. Slides were washed twice with PBT then processed according to the Epigenome NoE protocol PROT07 for hybridization.

DamID chromatin profiling

The Dam-Lamin and Dam alone constructs were previously described [S22, S23]. Dam-Wash was generated by PCR amplifying the full-length Wash cDNA (1-500 aa) as an 5'*Not*I-3'*Nhe*I fragment that was then cloned into the 5'*Not*I-3'*Xba*I sites of pNDamMyc vector to generate Dam-Wash(FL). Cells were transfected by electroporation. DamID chromatin profiling was performed as previously described [S17]. Dam-methylated DNA was hybridized on Nimblegen DM2 CGH arrays with a probe-spacing of ~300-bp. DamID profiles for each Dam fusion protein were performed in triplicate. Dam fusions were compared to the methylase alone to control for non-specific accessibility. Microarray data was processed as previously described [S24-S27]. All data processing and analysis was performed using the R package for statistical computing (http://www.r-project.org). Data was LOESS normalized and a custom R script was implemented to define overlapping domains, using a minimum 80% overlap threshold, where at least one domain had to have at least 80% overlap with the other. We used parameter optimization functions within CGTools to determine the transition threshold and proportion of positive probe thresholds. In short, sharp transitions in the DamID signal were identified using a sliding edge filter (window size 199 probes), and adjacent transitions exceeding a threshold (here 0.3) were combined into domains if at least 70% of the enclosed probes had a positive log2 ratio. Correlation plot were performed in Cistrome by comparing the averaged DamID signal for Wash and Lamin using the Lamin associated domains (LADs) identified in this study. Domain overlap was obtained in R by establishing the domains of Wash and previously reported LADs, which overlap the LADs generated on this study. P-values for overlapping domains were obtained using the R package *Cooccur* [S28].

M.SssI based chromatin accessibility assay

Although DamID chromatin profiles were obtained in Kc167 cells, we performed the chromatin accessibility experiments in S2R+ cells due their high knockdown efficiency. Chromatin accessibility was assayed as previously described [S29] with slight modifications. Briefly, $5x10^7$ cells were harvested and nuclei were prepared using Sucrose/NP40 buffer (supplemented with 1 mM PMSF and EDTA-free protease inhibitor cocktail (Roche)), then incubated for 5 min on ice and spun at 1500 xg. Nuclei were washed in Sucrose buffer without NP40 twice and three times

with M.SssI reaction buffer (New England Biolabs) and resuspended in 1 ml of M.SssI reaction buffer. 300 µl of isolated nuclei were treated with 60 U of M.SssI (New England Biolabs) for 25 min at 25°C. The reaction was immediately stopped by adding TENSK buffer (10 mM Tris pH 7.4, 1 mM EDTA, 150 mM NaCl, 1% SDS and 10 µg Proteinase K) and incubating at 55°C overnight. High molecular weight genomic DNA was isolated by standard methods and fragmented using a Bioruptor (Diagenode) to obtain an average fragment size of 500 bp. Methylated DNA immunoprecipitation (MeDIP) was performed by incubating 2 µg of fragmented DNA was denatured and immunoprecipitated with 2 µg of anti-5-methylcytosine (clone 33A3; Active Motif) for 2 hr at 4°C. Goat anti-mouse IgG-linked magnetic beads (Invitrogen) were used to recover the DNA/antibody complex and eluted in 0.1 mM Na_2HCO_3, 0.1% SDS and 2 µg of Proteinase K at 55°C overnight. Immunoprecipitated DNA was recovered with mini-elute PCR columns (Qiagen). DNA was amplified with WGA2 according to manufacturer's instructions (Sigma-Aldrich). Fully methylated DNA was obtained by recovering genomic DNA, sonicated to an average fragment size of 500 bp, treated twice with M.SssI *in vitro* and, for each biological replicate, an independent MeDIP with fully methylated DNA was performed as a control. DNA was labeled by random priming with Cy5- and Cy3-hexamers, and hybridized to a Nimblegen high-density 2.1M custom DM3 genome-wide tiling array [S30, S31] according to the manufacturer's protocol (Roche NimbleGen Inc.). To standardize for dynamic range differences, each Tukey-biweight normalized data set was transformed to a normalized z-score scale by converting the individual probe log2(IP/fully methylated DNA) values to standard deviates; z = (x - m)/s, where x = the log2 ratio of the probe, m = the mean of the data set, and s = the standard deviation of the data set [S32]. Triplicates were averaged and the background signal for each condition was evaluated by establishing the methylation signal of a 6000 random regions (2-3 Kb average). Random sequences were generated with the Excel-XSTAT plug-in. While mock and Wash RNAi presented similar baseline, the Lamin RNAi exhibited higher background levels globally suggesting a more global impact on chromatin accessibility upon Lamin depletion. To compare our dataset with the same baseline, the background noise was subtracted from each meta-analysis.

MeDIP-qPCR was performed as described previously [S24, S29]. After Proteinase K digestion, DNA was recovered with mini-elute PCR columns (Qiagen) in 150 µl of elution buffer. 2 µl of DNA was used per qPCR reaction. qPCR reactions were performed in triplicate and analyzed by fold enrichment based on a non-specific IgG using the following equation: $2^{(-(Ct\ Het\ 5mC - Ct\ Het\ IgG))}$. The values from heterochromatic regions were divided by the average signal of four promoter regions (Notch, Rel, Pc, Su(H)), which are not affected by Wash depletion (Figure 4A). Primers used for this study are listed below.

Bioinformatic Analyses

LiftOver to dm3 was applied to all dm2 genomic data. Meta-analyses were performed by aligning all regions at their 5' and 3' end and averaging the normalized probe values as a function of distance. Similar analyses were performed to all Drosophila Ref-seq genes at their transcriptional start sites and transcriptional termination sites. End analyses (meta-analysis) were performed as described [S31], by using custom scripts in R, or by using Galaxy/Cistrome [S33, S34]. Visualization was carried out using the UCSC browser [S35]. Developmental transcription

information was obtained from the UCSC browser. 6000 random sequences ranging between 1-5 Kb were generated in XLSTAT considering a similar number of binding site for regulatory elements uncovered by Filion et al. and Kharchenko et al. [S36, S37]. Additional Data Source: Chromatin states defined by the modENCODE Consortium [S1, S22] were obtained from: www.modencode.org/publications/integrative_fly_2010, [S1]; GSE22069 [S36], GSE5089 [S22].

Statistical Analyses

Prism Graphing Software was used to organize data, generate graphs, and perform statistical analysis. Unless otherwise indicated, the mean was graphed with error bars representing the standard error of the mean (± s.e.m.). Statistical analysis was performed using an unpaired t-test, with Welch's correction in cases where variance between data sets was significantly different. A $P<0.05$ was considered significant. For chromatin accessibility, statistical significance was determined using the two-sample KS test (non-parametric) in R on the average number of normalized signal within 1.5 kb at the ends of each region (1.5 kb downstream of the 5' end or upstream of the 3' end of each region).

Primers used in this study:

For RNAi

Lami1-F	GAATTAATACGACTCACTATAGGGAGAGCGGCTAATCAACGAGAAAG
Lami1-R	GAATTAATACGACTCACTATAGGGAGAGTAGAGCTGCTCATTGCCGT
Washi1-F	GAATTAATACGACTCACTATAGGGAGACTGGCCTGGGCATCCT
Washi1-R	GAATTAATACGACTCACTATAGGGAGAAAGGACATTGTCCCACACTC
Washi2-F	GAATTAATACGACTCACTATAGGGAGAATGGAGGAGTCACCTTAC
Washi2-R	GAATTAATACGACTCACTATAGGGAGAACATGGAAAAAGATGTCCGC
GFPi-F	GAATTAATACGACTCACTATAGGGAGAGGCACAAATTTTCTGTCAGT
GFPi-R	GAATTAATACGACTCACTATAGGGAGATCTGGTAAAAAGGACAGGGCC

For qPCR

HetAF1	ATGTTCGTCGGAAAAACGTC
HetAR1	TGGTAGACAGCGGAACAGTG
HetAF2	TGACCATGAGTGAAGGTGGA
HetAR2	TGGAACTCCCCAGAAAACAC
HetAF3	TGTCTTTTGGACCCTTGGAG
HetAR3	CCTTTGTTTCCCTCTTGTCG
HetAF4	TGCTCAGCCTGCTCTAATGA
HetAR4	TGGGCAGTCCTCTTTGTTGT
HetAF5	AGTTTATGCGTGTGCCTGTG
HetAR5	GCATGCGTCAGATGAACATT
HetBF6	CGTTACCAGGAAATGCGAGT
HetBR6	ACGATGATCTGCACACGAAG
HetBF7	CCGGCTAGGTAAACACATGG
HetBR7	TGGCGGGTAAGTGAAAAGAC

HetBF8	CCGATCGGAAATTGCTTTAC
HetBR8	GATCGGCAGTTTGTCGATTA
HetBF9	CGGTGACGTCTCTCAGTCAA
HetBR9	GCTCCGTAAGCAAAGCAATC
HetBF10	GACCCCAAAGTTTCTGCTCA
HetBR10	AATTCGCCGCTGTCTCTTTA
HetBF11	TATTGACGCACCTGTCCTTG
HetBR11	TCCTTGAATGGGTGGGATTA
NotchF	ACCGCTATGACGGCACTAAA
NotchR	TCTGTTTCAAATCGGCAGTG
Su(H)F	GAGCGCTAGTTGCAGCCTTA
Su(H)R	CAGCTGTCGTTTCTCTCACG
RelF	AGCAGTGGCGCACTAAAGTT
RelR	CGAGATGACTCACGGGTTTT
PcF	AGCACGGTAACTCTGCACCT
PcR	CTTGCCTCGACCAGTCATTT

Supplemental References

S1. Gerstein, M.B., Lu, Z.J., Van Nostrand, E.L., Cheng, C., Arshinoff, B.I., Liu, T., Yip, K.Y., Robilotto, R., Rechtsteiner, A., Ikegami, K., et al. (2010). Integrative analysis of the Caenorhabditis elegans genome by the modENCODE project. Science *330*, 1775-1787.

S2. Linardopoulou, E.V., Parghi, S.S., Friedman, C., Osborn, G.E., Parkhurst, S.M., and Trask, B.J. (2007). Human subtelomeric WASH genes encode a new subclass of the WASP family. PLoS genetics *3*, e237.

S3. Guillemin, K., Williams, T., and Krasnow, M.A. (2001). A nuclear lamin is required for cytoplasmic organization and egg polarity in Drosophila. Nature cell biology *3*, 848-851.

S4. Spradling, A.C. (1986). P element-mediated transformation, (Oxford: IRL Press).

S5. Cryderman, D.E., Morris, E.J., Biessmann, H., Elgin, S.C., and Wallrath, L.L. (1999). Silencing at Drosophila telomeres: nuclear organization and chromatin structure play critical roles. The EMBO journal *18*, 3724-3735.

S6. Dorer, D.R., and Henikoff, S. (1994). Expansions of transgene repeats cause heterochromatin formation and gene silencing in Drosophila. Cell *77*, 993-1002.

S7. Dorer, D.R., and Henikoff, S. (1997). Transgene repeat arrays interact with distant heterochromatin and cause silencing in cis and trans. Genetics *147*, 1181-1190.

S8. Sass, G.L., and Henikoff, S. (1998). Comparative analysis of position-effect variegation mutations in Drosophila melanogaster delineates the targets of modifiers. Genetics *148*, 733-741.

S9. Rodriguez-Mesa, E., Abreu-Blanco, M.T., Rosales-Nieves, A.E., and Parkhurst, S.M. (2012). Developmental expression of Drosophila Wiskott-Aldrich Syndrome family proteins. Dev Dyn *241*, 608-626.

S10. Reimer, G., Raska, I., Tan, E.M., and Scheer, U. (1987). Human autoantibodies: probes for nucleolus structure and function. Virchows Archiv. B, Cell pathology including molecular pathology *54*, 131-143.

S11. Liu, J.L., Wu, Z., Nizami, Z., Deryusheva, S., Rajendra, T.K., Beumer, K.J., Gao, H., Matera, A.G., Carroll, D., and Gall, J.G. (2009). Coilin is essential for Cajal body organization in Drosophila melanogaster. Molecular biology of the cell *20*, 1661-1670.

S12. Mendjan, S., Taipale, M., Kind, J., Holz, H., Gebhardt, P., Schelder, M., Vermeulen, M., Buscaino, A., Duncan, K., Mueller, J., et al. (2006). Nuclear pore components are involved in the transcriptional regulation of dosage compensation in Drosophila. Molecular cell *21*, 811-823.

S13. Meaburn, K.J., Gudla, P.R., Khan, S., Lockett, S.J., and Misteli, T. (2009). Disease-specific gene repositioning in breast cancer. The Journal of cell biology *187*, 801-812.

S14. Liu, R., Abreu-Blanco, M.T., Barry, K.C., Linardopoulou, E.V., Osborn, G.E., and Parkhurst, S.M. (2009). Wash functions downstream of Rho and links linear and branched actin nucleation factors. Development *136*, 2849-2860.

S15. Rosales-Nieves, A.E., Johndrow, J.E., Keller, L.C., Magie, C.R., Pinto-Santini, D.M., and Parkhurst, S.M. (2006). Coordination of microtubule and microfilament dynamics by Drosophila Rho1, Spire and Cappuccino. Nature cell biology *8*, 367-376.

S16. Shechter, D., Dormann, H.L., Allis, C.D., and Hake, S.B. (2007). Extraction, purification and analysis of histones. Nature protocols *2*, 1445-1457.

S17. Bianchi-Frias, D., Orian, A., Delrow, J.J., Vazquez, J., Rosales-Nieves, A.E., and Parkhurst, S.M. (2004). Hairy transcriptional repression targets and cofactor recruitment in Drosophila. PLoS biology *2*, E178.

S18. Andrew, D.J., and Scott, M.P. (1994). Immunological methods for mapping protein distributions on polytene chromosomes. Methods in cell biology *44*, 353-370.

S19. Agard, D.A., Hiraoka, Y., Shaw, P., and Sedat, J.W. (1989). Fluorescence microscopy in three dimensions. Methods in cell biology *30*, 353-377.

S20. Bantignies, F., Roure, V., Comet, I., Leblanc, B., Schuettengruber, B., Bonnet, J., Tixier, V., Mas, A., and Cavalli, G. (2011). Polycomb-dependent regulatory contacts between distant Hox loci in Drosophila. Cell *144*, 214-226.

S21. Peng, J.C., and Karpen, G.H. (2009). Heterochromatic genome stability requires regulators of histone H3 K9 methylation. PLoS genetics *5*, e1000435.

S22. Pickersgill, H., Kalverda, B., de Wit, E., Talhout, W., Fornerod, M., and van Steensel, B. (2006). Characterization of the Drosophila melanogaster genome at the nuclear lamina. Nature genetics *38*, 1005-1014.

S23. van Steensel, B., and Henikoff, S. (2000). Identification of in vivo DNA targets of chromatin proteins using tethered dam methyltransferase. Nature biotechnology *18*, 424-428.

S24. Weber, M., Davies, J.J., Wittig, D., Oakeley, E.J., Haase, M., Lam, W.L., and Schubeler, D. (2005). Chromosome-wide and promoter-specific analyses identify sites of differential DNA methylation in normal and transformed human cells. Nature genetics *37*, 853-862.

S25. Guelen, L., Pagie, L., Brasset, E., Meuleman, W., Faza, M.B., Talhout, W., Eussen, B.H., de Klein, A., Wessels, L., de Laat, W., et al. (2008). Domain organization of human chromosomes revealed by mapping of nuclear lamina interactions. Nature *453*, 948-951.

S26. van Bemmel, J.G., Pagie, L., Braunschweig, U., Brugman, W., Meuleman, W., Kerkhoven, R.M., and van Steensel, B. (2010). The insulator protein SU(HW) fine-tunes nuclear lamina interactions of the Drosophila genome. PloS one *5*, e15013.

S27. van Bemmel, J.G., Filion, G.J., Rosado, A., Talhout, W., de Haas, M., van Welsem, T., van Leeuwen, F., and van Steensel, B. (2013). A network model of the molecular organization of chromatin in Drosophila. Molecular cell *49*, 759-771.

S28. Huen, A.C., Park, J.K., Godsel, L.M., Chen, X., Bannon, L.J., Amargo, E.V., Hudson, T.Y., Mongiu, A.K., Leigh, I.M., Kelsell, D.P., et al. (2002). Intermediate filament-membrane attachments function synergistically with actin-dependent contacts to regulate intercellular adhesive strength. The Journal of cell biology *159*, 1005-1017.

S29. Bell, O., Schwaiger, M., Oakeley, E.J., Lienert, F., Beisel, C., Stadler, M.B., and Schubeler, D. (2010). Accessibility of the Drosophila genome discriminates PcG repression, H4K16 acetylation and replication timing. Nature structural & molecular biology *17*, 894-900.

S30. Mito, Y., Henikoff, J.G., and Henikoff, S. (2007). Histone replacement marks the boundaries of cis-regulatory domains. Science *315*, 1408-1411.

S31. Deal, R.B., Henikoff, J.G., and Henikoff, S. (2010). Genome-wide kinetics of nucleosome turnover determined by metabolic labeling of histones. Science *328*, 1161-1164.

S32. Conerly, M.L., Teves, S.S., Diolaiti, D., Ulrich, M., Eisenman, R.N., and Henikoff, S. (2010). Changes in H2A.Z occupancy and DNA methylation during B-cell lymphomagenesis. Genome research *20*, 1383-1390.

S33. Shin, H., Liu, T., Manrai, A.K., and Liu, X.S. (2009). CEAS: cis-regulatory element annotation system. Bioinformatics *25*, 2605-2606.

S34. Liu, T., Ortiz, J.A., Taing, L., Meyer, C.A., Lee, B., Zhang, Y., Shin, H., Wong, S.S., Ma, J., Lei, Y., et al. (2011). Cistrome: an integrative platform for transcriptional regulation studies. Genome biology *12*, R83.

S35. Karolchik, D., Barber, G.P., Casper, J., Clawson, H., Cline, M.S., Diekhans, M., Dreszer, T.R., Fujita, P.A., Guruvadoo, L., Haeussler, M., et al. (2014). The UCSC Genome Browser database: 2014 update. Nucleic acids research *42*, D764-770.

S36. Filion, G.J., van Bemmel, J.G., Braunschweig, U., Talhout, W., Kind, J., Ward, L.D., Brugman, W., de Castro, I.J., Kerkhoven, R.M., Bussemaker, H.J., et al. (2010). Systematic protein location mapping reveals five principal chromatin types in Drosophila cells. Cell *143*, 212-224.

S37. Kharchenko, P.V., Alekseyenko, A.A., Schwartz, Y.B., Minoda, A., Riddle, N.C., Ernst, J., Sabo, P.J., Larschan, E., Gorchakov, A.A., Gu, T., et al. (2011). Comprehensive analysis of the chromatin landscape in Drosophila melanogaster. Nature *471*, 480-485.